Desalination and Water Treatment
www.deswater.com
doi: 10.1080/19443994.2015.1072059

57 (2016) 15515–15523
July

Taylor & Francis
Taylor & Francis Group

Optimization of phosphorus removal from reject water of sludge thickening and dewatering process through struvite precipitation

Weichao Ren, Zhen Zhou*, Li Wan, Dalong Hu, Lu-Man Jiang, Luochun Wang

College of Environmental and Chemical Engineering, Shanghai University of Electric Power, Shanghai 200090, China, email: renweichao9265@163.com (W. Ren), Tel./Fax: +86 21 35303544; emails: zhouzhen@shiep.edu.cn (Z. Zhou), 332143738@qq.com (L. Wan), 594598637@qq.com (D. Hu), jiangluman@shiep.edu.cn (L.-M. Jiang), wangluochun@shiep.edu.cn (L. Wang)

Received 9 February 2015; Accepted 8 July 2015

ABSTRACT

Chemical precipitation using magnesium salt is an effective technology for recovering phosphorus and ammonium nitrogen from wastewater. Effects of pH, Mg/P ratio, stirring rate, and seed crystal (SC) dosage on phosphate removal efficiency (PRE) and average particle diameter (APD) of precipitates were investigated for reject water from sludge thickening and dewatering process in municipal wastewater treatment. Response surface methodology was applied to understand the significance and the interactive effects of reaction factors. The increases in Mg/P ratio, stirring rate, and SC dosage were in favor of phosphate removal from reject water. pH is the dominant factor for phosphate removal by magnesium, followed by Mg/P and stirring rate, while SC dosage has the least effect on PRE and APD. Kinetic analysis showed that both pH regulation and SC addition could accelerate the reaction rate. The optimum conditions were obtained at pH 10.4, Mg/P of 2.0, stirring rate of 150 rpm, and SC dosage of 26.7 mg/L, with PRE of 95.9%, APD of 104 μm, and final mass of precipitate of 936.3 mg/L. X-ray diffractometer analysis revealed that the increase in pH resulted in the increase in crystallinity and the conversion of struvite to calcium pyrophosphate, and the precipitates of reject water were struvite at pH < 10.5.

Keywords: Phosphorus removal; Reject water; Struvite; Sludge thickening and dewatering; Response surface methodology

1. Introduction

Reject water from municipal wastewater treatment is the liquid fraction produced in sludge thickening, digestion and dewatering units, and contains high concentrations of nitrogen (N) and phosphate (P) [1,2]. Although the flow rate of reject water is small (<5% of the total flow rate of influent wastewater) [3], it contributes to 10–50% of N load and from 10 to 80% of P load entering the activated sludge tank [2]. Therefore, effective treatment of reject water with high concentrations of N and P is necessary to meet standards of nutrient removal in wastewater treatment plants (WWTPs).

A successful method for nutrient removal from wastewater is simultaneous precipitation of soluble orthophosphate (PO_4^{3-}-P) and ammonium nitrogen (NH_4^+-N) in the form of struvite ($MgNH_4PO_4{\cdot}6H_2O$) using magnesium salt [4]. The struvite method has been applied to recover N and P from swine

*Corresponding author.

wastewater [5,6], coking wastewater [7], fertilizer wastewater [8], landfill leachate [9,10], urine [11], supernatant released from waste activated sludge [12,13], industrial anaerobic effluents [14,15], etc. The separation and recovery of struvite from reject water have also been extensively addressed and already implemented in full-scale WWTPs [16]. Nevertheless, most studies focused on P removal from anaerobic digester supernatant, but few on simultaneous N and P recovery from supernatant after sludge thickening and dewatering processes.

Although the influence of different parameters, molar ratio of Mg dosage and the concentration of phosphate in the reject water (Mg/P), mixing, pH, temperature, seed crystal (SC), competitive ions, etc. on phosphate removal by magnesium salt have been investigated [17–22], detailed information on interaction influence of process parameters on PO_4^{3-}-P removal efficiency (PRE) and particle size of precipitates was hardly found in the literature. This study focused on the influence of process parameters on P removal by magnesium salt in real reject water from the centrifugal thickening and dewatering process. The process parameters studied were pH, Mg/P, stirring rate, and SC dosage. The kinetics of P removal by struvite was also investigated. An experiment setup was established to study the influence of these variables on PRE and average particle diameter (APD) of precipitates crystal. The response surface methodology (RSM) was employed to maximize PRE and APD of precipitates crystal. The recovered precipitate was examined to evaluate struvite quality and to prove the presence of coprecipitate.

2. Materials and methods

2.1. Reject water

The reject water was taken from the centrifugal thickening and dewatering process of Bailonggang WWTP in Shanghai (China), which treats about 2,000,000 m^3/d of municipal wastewater using anaerobic–anoxic–aerobic process. The reject water was pre-sedimented for solid–liquid separation, and the liquid supernatant was used as an influent for precipitation. The characteristics of the pre-sedimented reject water are shown in Table 1. The magnesium sulfate ($MgSO_4{\cdot}7H_2O$) was used as magnesium source for phosphate removal because of its high solubility (71 g/100 ml at 20°C).

2.2. Batch tests and sampling

The batch tests were performed in a ZR4-6 Flocculator (Zhongrun Ltd, Shenzhen, China). Each ZR4-6 beaker was filled with 500 ml of reject water. The addition of $MgSO_4$ solution was carried out under continuous stirring at a faster speed for 2 min. Then, the stirring rate was maintained at the consigned value for 15 min. The pH was recorded using an HQ30d portable meter (Hach, USA). The precipitates were washed with deionized water and dried in an oven at 303 K that did not influence the nature of precipitates [5]. A mixed liquor sample of 30 ml was taken for particle analysis at the terminal of stirring period. After 30 min sedimentation, a 20 ml sample of supernatant was collected from beakers for dissolved compound analysis. In the test for analyzing phosphate removal kinetics by magnesium, the stirring time was prolonged to 120 min, and a 20 ml sample of supernatant was collected at presented intervals.

2.3. Analytical method

Concentrations of NH_4^+-N and PO_4^{3-}-P were measured according to standard methods [23]. The precipitates were characterized by D8 Advance Powder X-ray diffractometer (XRD) (40 kV, 40 mA, step size 0.1°, Bruker Ltd, Germany). The particle diameter of precipitate was measured by SALD-2201 laser diffraction particle size analyzer (SHIMADZU, Japan).

2.4. Experimental design

Precipitation process for reject water treatment was investigated by single factor and RSM experiment. The statistical design of experiments is an efficient procedure for planning experiments so that the data obtained can be analyzed to yield valid and objective conclusions. The experiments were designed against a three-level full factorial trial, which required a total of

Table 1
Characterization of the reject water

Index	pH	NH_4^+-N (mg/L)	PO_4^{3-}-P (mg/L)	Ca^{2+} (mg/L)	Mg^{2+} (mg/L)
Concentration	7.71 ± 0.18	272.10 ± 28.93	94.62 ± 10.25	94.61 ± 7.09	19.04 ± 1.82

29 runs with five central points. Four process parameters and selected ranges were determined: *A*, pH (X_1, 7–11); *B*, Mg/P (X_2, 0.5–2.0); *C*, stirring rate (X_3, 10–150 rpm); and *D*, SC dosage (X_4, 5–97 mg/L). The experimental levels of each variable were lower limit, median, and upper limit of the selected range. The PRE was selected as the response variable of pollutants removal because it is more sensitive than NH_4^+-N as the weight ratio of NH_4^+-N and PO_4^{3-}-P is 2.24 in struvite. The APD was also selected as response variable for the estimation of crystallinity.

2.5. Data evaluation

The RSM can be regarded as a collection of statistical and mathematical techniques useful for optimizing objective functions. The methodology is based on approximation of the objective function by a low-order polynomial on a small sub-region of the domain. Given a response variable Y and k factors, X_1, ... , X_k, the main purpose of RSM is to find the combination of factor levels to achieve the optimal response. For computational convenience, the variables are usually standardized to coded or design variables, x_1, … , x_k, so that the design center is at the point $(x_1, \ldots, x_k) = 0$.

The Box–Behnken modified plan uses a second-order polynomial model to predict the ionic concentration values as a function of a combination of the process parameters (pH, Mg/P, stirring rate, SC dosage).

$$Y = \beta_0 + \sum_{i=1}^{4} \beta_i X_i + \sum_{i<j} \beta_{ij} X_i X_j + \sum_{i=1}^{4} \beta_{ii} X_i^2 + \varepsilon \quad (1)$$

where Y is the predictive response. In this study, the responses were predicted and used for the optimization step. β_0 is the constant term, β_i is the coefficient of the linear parameters X_i (*A*, *B*, *C*, *D*), β_{ij} represents the coefficients of the interaction parameters X_i and X_j, and β_{ii} represents the coefficients of the quadratic parameters X_i^2 (*AA*, *BB*, *CC*, and *DD*) which show the quadratic dependence of the responses to a parameter.

2.6. Kinetics of phosphate removal by magnesium

As for the coprecipitation of phosphate, ammonium, and magnesium, the reaction rate of phosphate theoretically follows a third-order kinetic equation:

$$\frac{dx}{dt} = k_3(a-x)(b-x)(c-x) \quad (2)$$

where a (mol/L) is the initial dose of Mg^{2+}, b (mol/L), and c (mol/L) refer to initial concentrations of NH_4^+-N and PO_4^{3-}-P in the reject water, x (mol/L) is the concentration of phosphate reacted, k_3 [L^2/(mol^2 h)] is the third-order kinetic constant, and t (h) is the reaction time. In the reject water, the molar ratio of NH_4-N and PO_4^{3-}-P in the reject water was as high as 6.37, indicating $b >> x$ in Eq. (2). Therefore, Eq. (2) could be simplified as Eq. (3):

$$\frac{dx}{dt} = k_3 b(a-x)(c-x) \quad (3)$$

Integration of the Eq. (3) gives:

$$\ln\frac{a-x}{c-x} = kt - \ln\frac{a}{c} \quad (4)$$

where k [L^2/(mol^2 h)] is pseudo-second-order kinetic rate constant and equals to $k_3 b$.

3. Results and discussion

3.1. Single factor experiments

3.1.1. Effect of pH on phosphate removal

Fig. 1(a) presents the effect of pH on PRE of reject water at Mg/P ratio of 1.2 and stirring rate of 150 rpm. The PRE was increased from 2.3% at pH 6 to 92.3% at pH 10, and then decreased with further increase in pH. When pH was below 8, no visible precipitates were observed, and the PRE was very low (<15%). It was because the increase in H^+ concentration in the solution inhibited the struvite crystallization [18]. When pH > 10, the formation of $Mg_3(PO_4)_2$ occurred instead of struvite, which resulted in the decrease in PRE. If the pH continued to rise, the PRE was significantly decreased because of the generation of $Mg(OH)_2$. Gadekar and Pullammanappallil [24] showed that the pH maximizing struvite fraction in the precipitate was dependent on the initial molar ratio of ammonium, magnesium, and phosphate. At equimolar ratio, the optimum pH was 8.5. When ammonium was in excess, the optimum pH was 9.8, and the precipitate was predominantly struvite. In previous works concerning struvite precipitation of swine wastewater, a wide range of the optimum pH (8.0–10.5) [5,17,25] was reported.

3.1.2. Effect of initial Mg/P ratio on phosphate removal

In the reject water, low Mg/P molar ratio of 0.26 indicated that Mg was the limiting element for struvite precipitation, and external Mg should be dosed to enhance the degree of saturation [16].

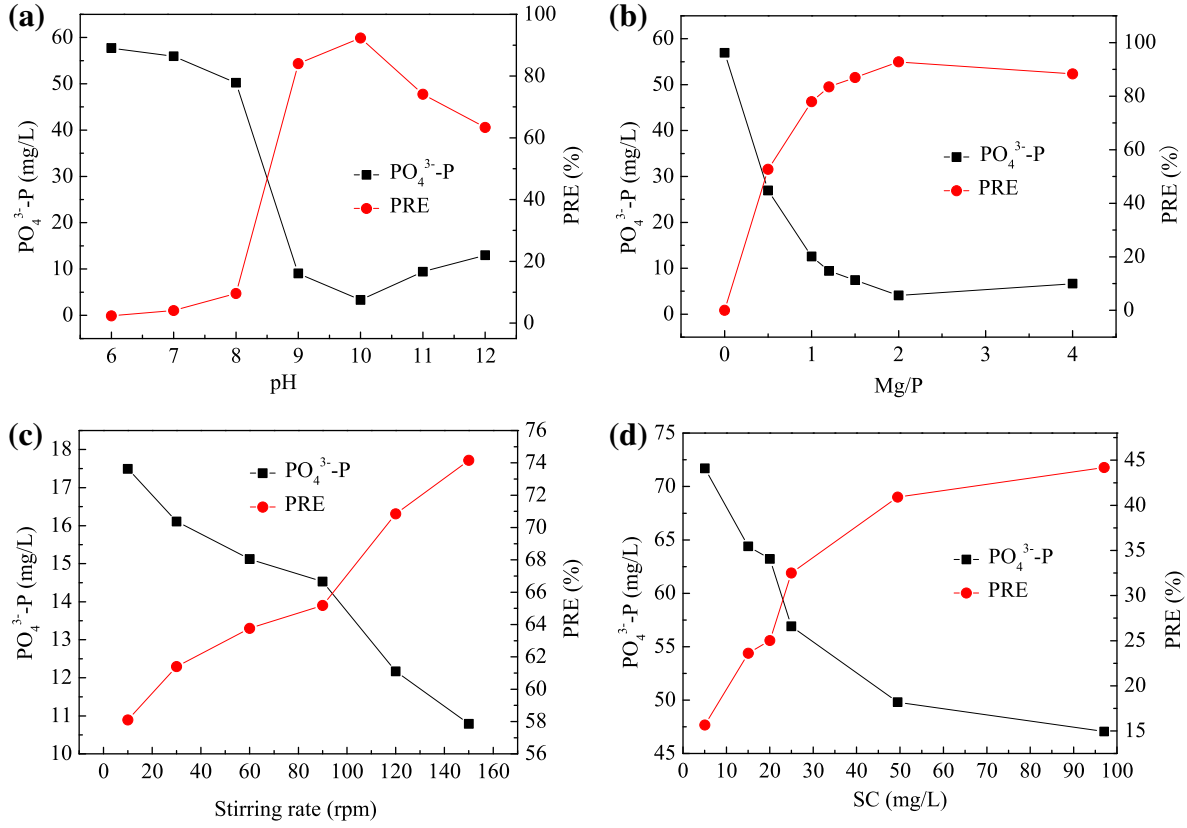

Fig. 1. Effect of pH (a), Mg/P ratio (b), stirring rate (c), and SC dosage (d) on phosphorus removal of reject water.

Fig. 1(b) illustrates the effect of initial Mg/P ratio on PRE of reject water at pH of 9.0 and stirring rate of 150 rpm. The PRE increased from 0 at Mg/P = 0 to 92.8% at Mg/P = 2, and then maintained constant at Mg/P > 2.0. The results were consistent with Song et al. [25], who also found that the PRE increased with the increase in Mg/P molar ratio. Nevertheless, the Mg/P ratio played an insignificant role on PRE with Mg/P ratio higher than 1.4 (Fig. 1(b)) in this study, which was within the reported range of 1.0–1.6 [26,27].

3.1.3. Effect of stirring rate on phosphate removal

Fig. 1(c) illustrates the effect of stirring rate on PRE of reject water at pH of 9.0 and Mg/P ratio of 1.2. The PRE increased from 58.1% at stirring rate of 10 rpm to 74.2% at stirring rate of 150 rpm, indicating that the stirring rate was not the main factor on PRE compared to pH and Mg/P ratio. Nevertheless, the stirring rate had a large influence on the formation of struvite, especially on the particle size of precipitates. With stirring rate increasing from 10 to 150 rpm, the APD decreased from 117.8 to 39.8 μm at pH of 9 and Mg/P ratio of 1.25.

3.1.4. Effect of SC dosage on phosphate removal

SC-induced crystallization has been recognized as an effective method to remove phosphate [19,20,28,29]. The pre-formed precipitate with APD of 40 μm was added to the reject water as SC in this study. Fig. 1(d) illustrates the effect of SC dosage on PRE of reject water at pH of 8.0, Mg/P ratio of 1.2, and stirring rate of 150 rpm. With SC dosage increasing from 5 to 97 mg/L, the PRE increased from 15.7 to 44.2% at pH of 8.0. Furthermore, the addition of SC accelerated the formation of precipitates, and the APD increased from 40.4 to 96.8 μm with the SC dosage increasing from 5 to 97 mg/L.

3.2. Effect of pH and SC on phosphate removal kinetics

The changes of $\ln[(a-x)/(c-x)]$ with time under different conditions are shown in Fig. 2. The high coefficients of determination ($R^2 > 0.95$) in the fit curve lend credibility to the simplified model (Eq. (4)). The pseudo-second-order kinetic rate constant increased from 0.41 to 0.72 h^{-1} after the addition of SC at pH 7. This showed that SC addition increased the apparent reaction rate and shortened the time to reach

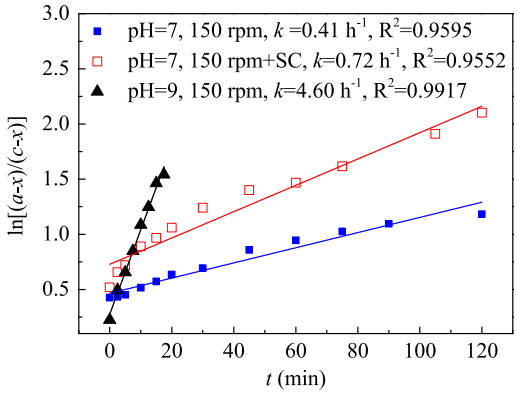

Fig. 2. The evolution of $\ln(a - x)/(c - x)$ follows pseudo-second-order kinetics.

equilibrium for precipitation. According to classical homogeneous nucleation theory, the crystal nucleus would grow into crystals only when the radius of crystal nucleus is higher than the critical radius. Therefore, SC addition of seeds as crystal nuclei would accelerate crystal growth by removing the need for the formation of crystal nuclei [20]. The k value significantly enhanced by more than 10 times with pH increasing from 7 to 9, suggesting that struvite crystallization was greatly promoted with the increase in pH at pH < 9.0 [18].

3.3. Response surface analysis

3.3.1. Phosphate removal is mainly influenced by pH and stirring rate

The RSM analysis can assist in the understanding and modeling of significant reaction factors and the interactive effects of multiple variables on PRE and APD from reject water by chemical precipitation. The regression analysis suggested that the quadratic model was the most appropriate one among all of the polynomial models for the simulation of PRE. The final empirical regression model in terms of coded factors for PRE was described as follows:

$$Y_{PRE} = 77.46 + 37.38A + 2.11B + 7.05C + 3.10D + 2.96AB + 0.56AC + 0.60AD + 11.77BC - 4.31BD - 0.070CD - 29.68A^2 - 7.76B^2 - 9.02C^2 - 0.83D^2 \quad (5)$$

An analysis of variance (ANOVA) was further applied to evaluate the significance and adequacy of the model, and identify the complex relationship between variables and responses. The reported statistical results are summarized in Table 2. Based on the lack of fit values (0.0565) and a very low Prob. > F values (≤0.0001) for both responses as presented in Table 2, "Adeq Precision" measured the signal-to-noise ratio and a ratio greater than 4 was considered desirable. The "Adeq Precision" ratio of 9.848 indicated an adequate signal. These showed that the quadratic model could be used to navigate the design space, and the good fitness and significance of the regression models can be concluded [30]. The pH and stirring rate were the dominant process parameters which had a positive influence on PRE (Table 2). The interaction between Mg/P and stirring rate was the most significant.

Table 2
ANOVA for PRE and APD

Process parameters	Prob. > F[a] for PRE	Prob. > F for APD
R^2	0.9091	0.7487
Model	<0.0001	0.0250
A: pH	<0.0001(+)[b]	0.9359(−)
B: Mg/P	0.5873(+)	0.8594(+)
C: stirring rate	0.0844(+)	0.8230(+)
D: SC dosage	0.4283(+)	0.5928(−)
AB	0.6592(+)	0.0005(−)
AC	0.9333(+)	0.7917(−)
AD	0.9292(+)	0.7753(−)
BC	0.0950(+)	0.4283(+)
BD	0.5223(−)	0.6711(+)
CD	0.9917(−)	0.9112(−)
A^2	<0.0001(−)	0.0031(+)
B^2	0.1552(−)	0.0908(+)
C^2	0.1024(−)	0.3154(−)
D^2	0.8751(−)	0.4142(−)
Lack of fit	0.0565	0.2363

[a]A low probability F value ("Prob. > F") less than 0.05 indicates that model term is significant.
[b](+) indicates a positive influence and (−) a negative influence on the studied responses.

Response surface plots were used to investigate the interaction effect of two factors on the PRE. Three-dimensional response surface plots of the predictive quadratic model for the PRE are shown in Fig. 3(a)–(c). Fig. 3(a) and (b) demonstrates that at lower pH level, the PRE was lower. U-shaped plots suggested that a suitable pH could benefit PRE, which was consistent with the results of single factor analysis. Compared to pH, Mg/P and SC dosage almost had no effect on phosphate removal. The reason was that when Mg/P was 0.5, PRE was already high. At low pH, SC addition will promote PRE. Fig. 3(c) demonstrates that the stirring rate and Mg/P have antagonistic effects on PRE. Lower PRE was yielded

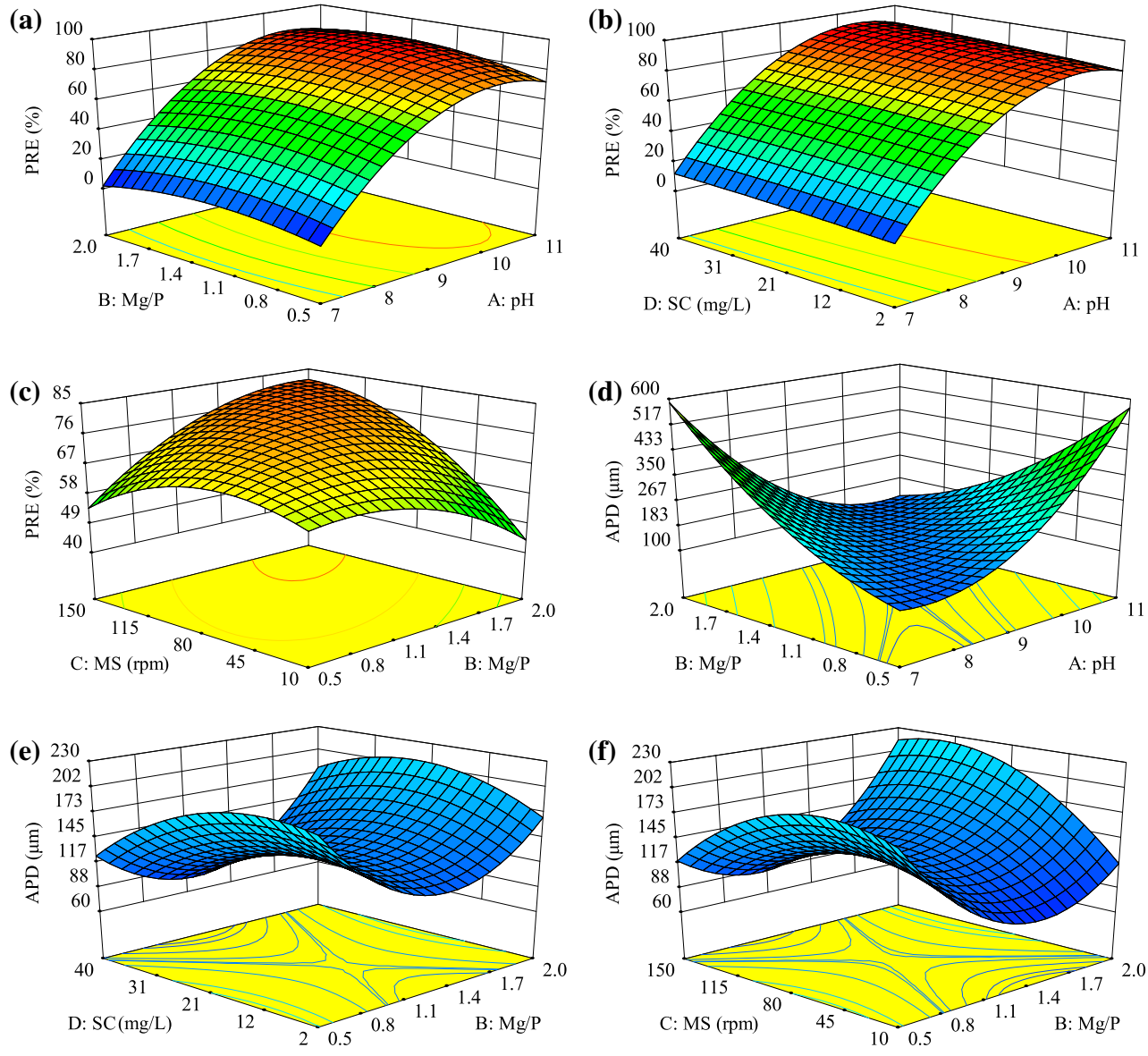

Fig. 3. Response surface plots for the combined effects on PRE (a–c) and APD (d–f): (a/d) stirring rate = 80 rpm, SC dosage = 51 mg/L; (b/e) Mg/P = 1.25, stirring rate = 80 rpm; (c/f) pH 9.0, SC dosage = 51 mg/L.

in the region of low stirring rate and high Mg/P, or high stirring rate and low Mg/P.

3.3.2. APD is mainly influenced by SC dosage

The final quadratic regression model in terms of coded factors for APD was described as follows:

$$Y_{APD} = 129.12 - 2.45A + 5.39B + 6.29C - 16.36D - 232.36AB - 13.94AC - 15.07AD + 42.23BC + 22.45BD - 5.88CD + 145.01A^2 + 73.84B^2 - 42.34C^2 - 34.21D^2 \quad (6)$$

The reported statistical results are summarized in Table 2. Based on the lack of fit values (0.2363) and a low Prob. > F values (0.0250) for both responses as presented in Table 2, the "Adeq Precision" ratio of 7.426 indicated an adequate signal, good fitness, and significance of the regression models. SC dosage was the leading process parameter affecting the APD (Table 2). Dosing the appropriate amount of SC could help with particles growth, but excess SC was not in favor of particles growth.

The response surface plots of the predictive quadratic model for the APD are shown in Fig. 3(d)–(f). Fig. 3(d) shows that pH and Mg/P have antagonistic

effects on APD. Large precipitate particles (high APD) were obtained in the region of low pH and high Mg/P, or high pH and low Mg/P. Considering the PRE in Fig. 3(a), the condition of high pH and low Mg/P ratio could generate products with high APD and obtain high PRE. Fig. 3(e) and (f) demonstrates that the combined effects of Mg/P, stirring rate, and SC dosage were not obvious.

3.3.3. Selection of optimal levels and estimation of optimum response characteristics

The aim of the work was to maximize PRE and to yield precipitates with largest particles. The predicted optimal results for PRE were obtained using the pH of 10.4, Mg/P ratio of 2.0, stirring rate of 150 rpm, and SC dosage of 26.7 mg/L, resulting in 95.9% (with 95% confidence intervals of 89–104%) of PRE. The APD under this condition was 104 μm. To verify the model adequacy, these optimum values were checked experimentally which resulted in 95.2 ± 1.0% of PRE and 108 μm of APD by struvite precipitation. A good correlation between these two results verified the validity of the response model and the existence of an optimal point.

Under the optimized conditions, the final mass of harvested precipitates was 936.3 mg/L by deducting SC dosage. According to phosphorus removal of the reject water, the theoretical yield of $MgNH_4PO_4{\cdot}6H_2O$ was 713.8 mg/L, and thus the purity of harvested precipitates was 76.3%. The results indicated that organic and impurity substances (i.e. calcium, carbonate) in the reject water were coprecipitated with struvite.

3.4. XRD analysis of precipitates

XRD patterns of precipitates in Fig. 4 show that the degree of crystallinity increased with pH rising from 8.5 to 11.5. Struvite formed at pH 8.5 although it was poorly crystalline as indicated by struvite-derived peaks (PDF#15-0762) (Fig. 4(a)). At pH 9.5, the precipitate was also mainly struvite with higher degree of crystallinity. The coexistence of struvite, $Ca_2P_2O_7$ (PDF#23-0871#), and $Mg_3(PO_4)_2$ (PDF#35-0134) was observed at pH 10.5 (Fig. 4(c)). At pH 10.5, peaks of struvite became weak, and new peaks at 31.6˚, 45.3˚, and 56.3˚ appeared. These new peaks matched well with $Ca_2P_2O_7$ (PDF#23-0871#). The increase in pH from 8.5 to 10.5 resulted in the partial conversion of struvite to $Mg_3(PO_4)_2$ and $Ca_2P_2O_7$ complexes. Zhou and Wu [31] have shown that the precipitated crystal was struvite, $Mg_3(PO_4)_2$, and $MgHPO_4{\cdot}3H_2O$ at pH 10.12, Mg/N/P = 1.16/1/1.54. In Fig. 4(d), the peaks of struvite and $Mg_3(PO_4)_2$ which were related to magnesium

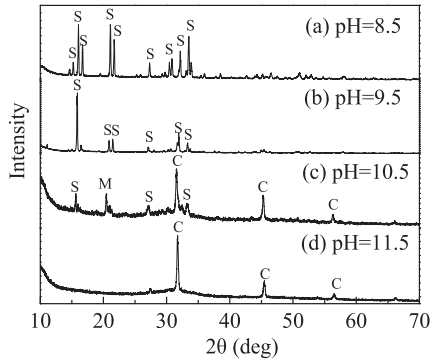

Fig. 4. XRD patterns of precipitates obtained under different pHs. (Mg/P = 1.2, 150 rpm). The peaks are labeled S, struvite; C, calcium pyrophosphate ($Ca_2P_2O_7$); and M, magnesium phosphate ($Mg_3(PO_4)_2$).

disappeared, and chiefly the strong peaks associated with $Ca_2P_2O_7$ appeared owing to the existence of Ca^{2+} in the reject water. The studies of Le Corre et al. [32] and Wang et al. [33] have indicated that the high Ca^{2+} in the solutions could lead to the formation of calcium phosphates, which would decrease the amount of struvite and PRE. Hao et al. [34] also found that the Ca^{2+} began to appear in the precipitate when pH > 8.5, and with the increase in pH, Mg^{2+} precipitated in the form of $Mg_3(PO_4)_2$ and $Mg(OH)_2$.

4. Conclusions

Effects of pH, Mg/P ratio, stirring rate, and SC dosage on PRE, and the particle size of precipitates were investigated for reject water from sludge thickening and dewatering process. RSM was applied to assist in understanding the significance and the interactive effects of reaction factors. The increases in Mg/P ratio, stirring rate, and SC dosage were in favor of phosphate removal from reject water, and adding SC and increasing pH could shorten the time to reach equilibrium. After the RSM optimization, the optimum conditions were obtained at pH 10.4, Mg/P of 2.0, stirring rate of 150 rpm, and SC dosage of 26.7 mg/L, with PRE of 95.9%, APD of 104 μm, and final mass of precipitate of 936.3 mg/L. XRD analysis revealed that the increase in pH resulted in the increase in crystallinity and the conversion of struvite to calcium pyrophosphate, and the precipitates of reject water were struvite at pH < 10.5.

Acknowledgment

This work was financially supported by the National High-tech R&D Program (863 Program) of China (No. 2012AA063403).

References

[1] B. Karwowska, E. Sperczyńska, E. Wiśniowska, Characteristics of reject waters and condensates generated during drying of sewage sludge from selected wastewater treatment plants, Desalin. Water Treat. (2014) 1–8.

[2] A.R. Pitman, Management of biological nutrient removal plant sludges—Change the paradigms?, Water Res. 33 (1999) 1141–1146.

[3] C.H. Guo, V. Stabnikov, V. Ivanov, The removal of nitrogen and phosphorus from reject water of municipal wastewater treatment plant using ferric and nitrate bioreductions, Bioresour. Technol. 101 (2010) 3992–3999.

[4] Y. Liu, S. Kumar, J.H. Kwag, C. Ra, Magnesium ammonium phosphate formation, recovery and its application as valuable resources: A review, J. Chem. Technol. Biotechnol. 88 (2013) 181–189.

[5] E.L. Foletto, W.R.B.d. Santos, S.L. Jahn, M.M. Bassaco, M.A. Mazutti, A. Cancelier, A. Gündel, Organic pollutants removal and recovery from animal wastewater by mesoporous struvite precipitation, Desalin. Water Treat. 51 (2013) 2776–2780.

[6] Q. Lin, Z. Chen, J. Liu, B. Tang, J. Ye, L. Zhang, Optimization of struvite crystallization to recover nutrients from raw swine wastewater, Desalin. Water Treat. (2014) 1–7.

[7] T. Zhang, Q. Li, L. Ding, H. Ren, K. Xu, Y. Wu, D. Sheng, Modeling assessment for ammonium nitrogen recovery from wastewater by chemical precipitation, J. Environ. Sci. 23 (2011) 881–890.

[8] L. Ouchah, L. Mandi, F. Berrekhis, N. Ouazzani, Essays of phosphorus recovery into struvite from fertilizer industry effluents, Desalin. Water Treat. 52 (2013) 2886–2892.

[9] T. Zhang, L. Ding, H. Ren, Pretreatment of ammonium removal from landfill leachate by chemical precipitation, J. Hazard. Mater. 166 (2009) 911–915.

[10] S. Hassidou, T. Ismail, B.A. Mohamed, Phosphorus removal from Tunisian landfill leachate through struvite precipitation under controlled degassing technique, Desalin. Water Treat. 21 (2010) 295–302.

[11] P. Jin, W. Ren, C. Liang, X. Wang, L. Zhang, The study on the separate collection and nutrients recovery of urine in municipal wastewater, Desalin. Water Treat. 52 (2013) 5031–5036.

[12] J. Tong, Y. Chen, Recovery of nitrogen and phosphorus from alkaline fermentation liquid of waste activated sludge and application of the fermentation liquid to promote biological municipal wastewater treatment, Water Res. 43 (2009) 2969–2976.

[13] A.A. Ahmad, A. Idris, Release and recovery of phosphorus from wastewater treatment sludge via struvite precipitation, Desalin. Water Treat. 52 (2013) 5696–5703.

[14] M. Carballa, W. Moerman, W. De Windt, H. Grootaerd, W. Verstraete, Strategies to optimize phosphate removal from industrial anaerobic effluents by magnesium ammonium phosphate (MAP) production, J. Chem. Technol. Biotechnol. 84 (2009) 63–68.

[15] D. Hidalgo, F. Corona, J.M. Martín-Marroquín, J. del Álamo, A. Aguado, Resource recovery from anaerobic digestate: struvite crystallization versus ammonia stripping, Desalin. Water Treat. (2015) 1–7.

[16] K.V. Lo, F.A. Koch, Donald S Mavinic, K. Lo, Phosphorus recovery from anaerobic digester supernatants using a pilot-scale struvite crystallization process, J. Environ. Eng. Sci. 6 (2007) 561–571.

[17] G.W. Fernandes, A. Kunz, R.L.R. Steinmetz, A. Szogi, M. Vanotti, É.M. de Moraes Flores, V.L. Dressler, Chemical phosphorus removal: A clean strategy for piggery wastewater management in Brazil, Environ. Technol. 33 (2012) 1677–1683.

[18] H. Huang, C. Xu, W. Zhang, Removal of nutrients from piggery wastewater using struvite precipitation and pyrogenation technology, Bioresour. Technol. 102 (2011) 2523–2528.

[19] L. Qiu, G. Wang, S. Zhang, Z. Yang, Y. Li, An approach for phosphate removal with quartz sand, ceramsite, blast furnace slag and steel slag as seed crystal, Water Sci. Technol. 65 (2012) 1048–1053.

[20] Z. Liu, Q. Zhao, L. Wei, D. Wu, L. Ma, Effect of struvite seed crystal on MAP crystallization, J. Chem. Technol. Biotechnol. 86 (2011) 1394–1398.

[21] N.Y. Acelas, E. Flórez, D. López, Phosphorus recovery through struvite precipitation from wastewater: Effect of the competitive ions, Desalin. Water Treat. 54 (2015) 2468–2479.

[22] N.-M. Chong, Q.-M. Thai, Optimization and kinetics of nutrient removal from wastewater by chemical precipitation of struvite, Desalin. Water Treat. 54 (2015) 3422–3431.

[23] N.E.P.A. Chinese, Water and Wastewater Monitoring Methods, fourth ed., Chinese Environmental Science Publishing House, Beijing, China, 2012.

[24] S. Gadekar, P. Pullammanappallil, Validation and applications of a chemical equilibrium model for struvite precipitation, Environ. Model. Assess. 15 (2010) 201–209.

[25] Y. Song, P. Yuan, B. Zheng, J. Peng, F. Yuan, Y. Gao, Nutrients removal and recovery by crystallization of magnesium ammonium phosphate from synthetic swine wastewater, Chemosphere 69 (2007) 319–324.

[26] E. Diamadopoulos, K. Megalou, M. Georgiou, N. Gizgis, Coagulation and precipitation as post-treatment of anaerobically treated primary municipal wastewater, Water Environ. Res. 79 (2007) 131–139.

[27] M. Yoshino, M. Yao, H. Tsuno, I. Somiya, Removal and recovery of phosphate and ammonium as struvite from supernatant in anaerobic digestion, Water Sci. Technol. 48 (2003) 171–178.

[28] H. Huang, X. Xiao, L. Yang, B. Yan, Recovery of nitrogen from saponification wastewater by struvite precipitation, Water Sci. Technol. 61 (2010) 2741–2748.

[29] R. Yu, J. Geng, H. Ren, Y. Wang, K. Xu, Combination of struvite pyrolysate recycling with mixed-base technology for removing ammonium from fertilizer wastewater, Bioresour. Technol. 124 (2012) 292–298.

[30] M.A. Ahmad, R. Alrozi, Optimization of preparation conditions for mangosteen peel-based activated carbons for the removal of Remazol Brilliant Blue R using response surface methodology, Chem. Eng. J. 165 (2010) 883–890.

[31] S. Zhou, Y. Wu, Improving the prediction of ammonium nitrogen removal through struvite precipitation, Environ. Sci. Pollut. Res. 19 (2012) 347–360.
[32] K.S. Le Corre, E. Valsami-Jones, P. Hobbs, S.A. Parsons, Impact of calcium on struvite crystal size, shape and purity, J. Cryst. Growth 283 (2005) 514–522.
[33] J. Wang, J.G. Burken, X. Zhang, R. Surampalli, Engineered struvite precipitation: Impacts of component-ion molar ratios and pH, J. Environ. Eng. 131 (2005) 1433–1440.
[34] X. Hao, C. Wang, L. Lan, M. van Loosdrecht, Struvite formation, analytical methods and effects of pH and Ca^{2+}, Water Sci. Technol. 58 (2008) 1687–1692.